

# Quasinormal Modes of Extremal Reissner-Nordström Black Holes via Seiberg-Witten Quantization

---

Yi-Rong Wang,<sup>a</sup> Peng Yang,<sup>a</sup> and Kilar Zhang<sup>a,b,c,1</sup>

<sup>a</sup>*Department of Physics and Institute for Quantum Science and Technology, Shanghai University, 99 Shangda Road, Shanghai 200444, China*

<sup>b</sup>*Shanghai Key Lab for Astrophysics, Shanghai Normal University, 100 Guilin Road, Shanghai 200234, China*

<sup>c</sup>*Shanghai Key Laboratory of High Temperature Superconductors, Shanghai 200444, China*  
*E-mail: [wyr2024@shu.edu.cn](mailto:wyr2024@shu.edu.cn), [yangpeng522@shu.edu.cn](mailto:yangpeng522@shu.edu.cn), [kilar@shu.edu.cn](mailto:kilar@shu.edu.cn)*

**ABSTRACT:** We study the neutral scalar perturbations of asymptotically flat extremal Reissner-Nordström black holes via the quantum geometry of  $\mathcal{N} = 2$  SU(2) gauge theory with  $N_f = 2$  flavors. The master equation, given by a double confluent Heun equation, is mapped to the quantum Seiberg-Witten curve in the Nekrasov-Shatashvili limit. We compute the quasinormal mode frequencies non-perturbatively using the quantization condition derived from the Nekrasov-Shatashvili free energy. Our analytical results accurately reproduce the numerical benchmarks for massless fields, and capture the quasi-resonance behavior of massive probes at the strict extremal limit.

---

<sup>1</sup>Corresponding Author.

---

## Contents

|          |  |           |
|----------|--|-----------|
| <b>1</b> | <b>Introduction</b>  | <b>1</b>  |
| <b>2</b> | <b>Quantum Seiberg-Witten Geometry with <math>N_f = 2</math></b> | <b>4</b>  |
| <b>3</b> | <b>Scalar Perturbations of Extremal RN Black Holes</b>           | <b>5</b>  |
| 3.1      | Scalar Perturbations in the Extremal Background                  | 5         |
| 3.2      | Reduction to the Double Confluent Heun Equation                  | 6         |
| 3.3      | Branch Selection and the Parameter Dictionary                    | 7         |
| <b>4</b> | <b>Evaluation and Discussion</b>                                 | <b>8</b>  |
| 4.1      | Neutral Massless Scalar Perturbations                            | 8         |
| 4.2      | Neutral Massive Scalar Perturbations                             | 9         |
| <b>5</b> | <b>Conclusion and Outlook</b>                                    | <b>12</b> |
| <b>A</b> | <b>Nekrasov-Shatashvili Free Energy for <math>N_f = 2</math></b> | <b>13</b> |
| A.1      | Combinatorial Formulation  | 13        |
| A.2      | Full Free Energy and Instanton Expansion                         | 14        |
| A.3      | Quantum Mirror Map via Matone Relation                           | 15        |

---

## 1 Introduction

Since the seminal work of Seiberg and Witten in the 1990s [1, 2], the study of four-dimensional  $\mathcal{N} = 2$  supersymmetric Yang-Mills (SYM) theories has served as a paradigmatic framework for understanding strong coupling dynamics in quantum field theory [3, 4]. By exploiting the constraints imposed by holomorphy and electromagnetic duality, Seiberg-Witten (SW) theory successfully reduces the computation of the low-energy effective action to the geometric analysis of Riemann surfaces (SW curves) and their moduli spaces [5, 6]. This breakthrough not only unveiled the deep non-perturbative structure of gauge theories, further elucidated by Nekrasov’s partition functions [7], but also established profound connections with classical integrable systems [8], matrix models [9], and two-dimensional conformal field theories via the AGT correspondence [10, 11].

In the realm of gravitational physics, black hole perturbation theory remains a cornerstone for probing spacetime geometry and testing the predictions of general relativity [12, 13]. The relaxation process of a perturbed black hole is characterized

by its spectrum of complex frequencies, known as quasinormal mode (QNM) [14–16]. These modes act as the unique “fingerprints” of the black hole; their frequencies encode essential information about its mass, charge, and angular momentum, and are entirely independent of the initial perturbation.

With the advent of gravitational wave astronomy, the study of QNM has transitioned from a theoretical abstraction to an observational reality. The LIGO and Virgo collaborations have successfully detected the “ringdown” phase of binary black hole mergers—the stage where the remnant black hole radiates away distortions via gravitational waves [17, 18]. By analyzing the frequencies and damping times of these signals, physicists can perform “black hole spectroscopy” [19, 20] to rigorously test the No-Hair “theorem” [21], and search for potential deviations from general relativity [22, 23]. For isolated black holes in asymptotically flat spacetimes, QNM are fundamental observables that characterize their classical stability and late-time dynamical evolution [24].

Despite their physical importance, computing QNM analytically is notoriously difficult. The perturbation equations typically take the form of highly coupled systems of differential equations with complex effective potentials. Traditional approaches often rely on semi-analytic techniques and numerical root-finding routines (e.g., Leaver’s continued fraction method [25]), or asymptotic approximations like the WKB method [26, 27]. While effective for numerical evaluation, these conventional methods do not directly reveal the underlying analytic structure of the eigenvalue problem, making it challenging to provide an exact, geometrically motivated quantization condition. Furthermore, these methods encounter degeneracies or precision loss when dealing with coalescing singularities, such as those inherently arising in the strict extremal black hole limit, hence it is elusive to smoothly track fundamental modes into the quasi-resonance regime.

Since 2020, a novel analytical framework bridging black hole perturbation theory and quantum SW geometry, named the SW/QNM correspondence, has been established [28–31]. The mathematical foundation of this duality lies in the observation that the master equations governing black hole perturbations (e.g., the Teukolsky equation [32]), upon appropriate transformation, can be mapped to the Heun class of differential equations [33, 34]. These are precisely the quantum versions of the Picard-Fuchs equations associated with SW curves. This correspondence provides a precise “dictionary” that maps black hole parameters to gauge theory quantities, transforming the gravitational eigenvalue problem into a solvable problem in quantum integrable systems using Nekrasov partition functions. In the gauge theory side, the hypermultiplets with  $N_f$  flavors are associated with mass parameters  $m = \{m_1, \dots, m_{N_f}\}$  that encode the physical properties of the black hole, such as its dimension and asymptotic geometry. More recently, this framework is integrated into a broader classification of differential structures known as the extended Heun hierarchy, providing a systematic approach to the quantum geometry of SW

theories [35, 36].

In this paper, we apply this analytic framework to the extremal Reissner-Nordström (RN) black hole in asymptotically flat spacetime [37]. Extremal black holes are of particular interest in theoretical physics as they serve as zero-temperature ground states of charged black holes and represent the boundary of physically allowed states saturating the cosmic censorship bound. However, from the perspective of spectral analysis, the extremal limit is singular: the coalescence of the inner and outer horizons modifies the singularity structure of the underlying differential equation from a confluent Heun equation (CHE, typical for non-extremal cases) to a double confluent Heun equation (DCHE). This structural change implies that the relevant gauge theory dual for the asymptotically flat extremal RN black hole is distinct from the  $N_f = 3$  or  $N_f = 4$  theories associated with standard Kerr, Kerr-de Sitter, or non-extremal RN geometries [38, 39]. Instead, it corresponds to the  $SU(2)$  SW theory with  $N_f = 2$  fundamental hypermultiplets.

We construct an exact dictionary for the scalar perturbation in the asymptotically flat extremal RN background, mapping it to the quantum SW curve of the  $N_f = 2$  theory. Within this mapping, we explicitly identify a branch selection rule that is essential for imposing the correct boundary conditions characteristic of QNM—namely, purely ingoing waves at the horizon and purely outgoing waves at spatial infinity. This physical subtlety is critical for the consistency of the geometric correspondence.

Furthermore, we perform a non-perturbative computation of the QNM frequencies for the neutral scalar ( $q = 0$ ) case, utilizing the exact quantization condition derived from the Nekrasov-Shatashvili (NS) free energy [40]. For the neutral massless case ( $m_p = 0$ ), we demonstrate that the instanton expansion (evaluated up to the 12-instanton order) yields analytical predictions that are in agreement with high-precision numerical benchmarks [41]. For neutral massive fields ( $m_p \neq 0$ ), our framework allows to smoothly track the fundamental mode into the quasi-resonance regime ( $\text{Im}(\omega) \rightarrow 0$ ), resolving the singularity coalescence that plagues traditional methods at the strict extremal limit. Regarding charged scalar fields ( $q \neq 0$ ), the accuracy of current approaches need to be improved, and we leave it for future investigation.

The organization of this paper is as follows. In section 2, we review the quantum geometry of the SW theory and the associated quantization conditions. Section 3 systematically constructs the dictionary between the extremal RN black hole scalar perturbations and the quantum SW curve. Section 4 presents the validation of our results, and performs the quasi-resonance tracking. Finally, section 5 provides a summary and outlines future research directions. Appendix A details the definition and expansion of the NS free energy.

## 2 Quantum Seiberg-Witten Geometry with $N_f = 2$

In this section, we briefly review the essential dictionary relating SW theory to spectral theory, following [28]. We outline the geometric framework emerging from the NS limit, focusing specifically on the  $N_f = 2$  theory relevant for the extremal RN black hole. Central to this framework is the concept of *quantum periods*, which generalize the classical SW geometry to the quantum regime, thereby allowing for the exact computation of discrete spectral frequencies.

Consider a quantum operator  $H(\hat{x}, \hat{p})$  satisfying the canonical commutation relation  $[\hat{x}, \hat{p}] = i\hbar$ . Associated with this operator is a classical curve defined by  $H(x, p) = E$  and a differential one-form  $\lambda = p dx$ . The classical periods are defined by integrating  $\lambda$  along the non-trivial cycles of the curve, analogous to the SW periods in  $\mathcal{N} = 2$  gauge theory. To transit to the quantum regime, these classical periods are promoted to quantum periods via the WKB expansion:

$$\Pi^{\text{WKB}}(E, \hbar) = \sum_{n \geq 0} \hbar^n \oint_{\gamma} Q_n(x, E) dx. \quad (2.1)$$

Here, the functions  $Q_n(x, E)$  represent the expansion coefficients of the quantum differential  $\lambda(x, E, \hbar) = \sum_{n \geq 0} \hbar^n Q_n(x, E) dx$ . This quantum differential is formally constructed such that the exponential of its integral yields the wavefunction satisfying the quantum spectral equation,  $(H(\hat{x}, \hat{p}) - E) \exp\left[\frac{i}{\hbar} \int^x \lambda(y, E, \hbar)\right] = 0$ . Since the standard WKB series is typically asymptotic and divergent, a non-perturbative definition is required. The exact quantum periods are non-perturbatively determined by the NS free energy of the corresponding supersymmetric gauge theory [40, 42]. For the SU(2) theory, the quantum periods  $\Pi_A^{(N_f)}$  and  $\Pi_B^{(N_f)}$  associated with the A-cycle and B-cycle are given by:

$$\begin{aligned} \Pi_A^{(N_f)}(E, \mathbf{m}, \Lambda_{N_f}, \hbar) &= a(E, \mathbf{m}, \Lambda_{N_f}, \hbar), \\ \Pi_B^{(N_f)}(E, \mathbf{m}, \Lambda_{N_f}, \hbar) &= \left. \frac{\partial \mathcal{F}^{(N_f)}(a, \mathbf{m}, \Lambda_{N_f}, \hbar)}{\partial a} \right|_{a=a(E, \mathbf{m}, \Lambda_{N_f}, \hbar)}. \end{aligned} \quad (2.2)$$

Here,  $a$  is the scalar vacuum expectation value (Coulomb branch parameter),  $\mathbf{m}$  denotes the hypermultiplet masses, and  $\Lambda_{N_f}$  is the dynamical scale of the theory. The function  $\mathcal{F}^{(N_f)}$  is the NS free energy, which can be computed exactly using instanton counting techniques [40]. For the explicit combinatorial definitions and the instanton expansion for the  $N_f = 2$  case, we refer the reader to Appendix A.

Consequently, the exact quantization condition for the spectral problem is formulated as a Bohr-Sommerfeld-like condition involving the quantum B-period:

$$\Pi_B^{(N_f)}(E, \mathbf{m}, \Lambda_{N_f}, \hbar) = \mathcal{N}_B \hbar \left( n + \frac{1}{2} \right), \quad n = 0, 1, 2, \dots, \quad (2.3)$$

where  $\mathcal{N}_B$  is a numerical constant depending on the specific normalization of the cycles ( $2\pi$  in our convention).

This formalism provides a unified framework for various spectral problems, where the quantum SW curves for SU(2) gauge theories with  $N_f$  fundamental hypermultiplets naturally map to specific families of Heun equations (HE). While the initial finding [28] already analyzed the  $N_f = 2$  (DCHE) case in the extremal limit of the Kerr black hole, subsequent literature has predominantly focused on the extensive exploration of the  $N_f = 3$  (CHE) and  $N_f = 4$  (General Heun) scenarios (see e.g., [43–45]). To the best of our knowledge, the exact correspondence between the  $N_f = 2$  gauge theory and the extremal RN black hole remains unexplored. In this paper, we bridge this gap by establishing this exact mapping and providing the first analytic computation of quasinormal modes for the extremal RN geometry using this framework.

The quantum curve for the  $N_f = 2$  theory takes the form of the DCHE. It can be written as a Schrödinger-like equation:

$$\hbar^2 \Psi''(z) + \widehat{Q}_2(z) \Psi(z) = 0, \quad (2.4)$$

with the potential given by:

$$\widehat{Q}_2(z) = -\frac{\Lambda_2^2}{16} - \frac{m_1 \Lambda_2}{2z} + \frac{4E + \hbar^2}{4z^2} - \frac{m_2 \Lambda_2}{2z^3} - \frac{\Lambda_2^2}{16z^4}. \quad (2.5)$$

This geometric/gauge-theoretic perspective not only resums the divergent WKB series but also provides the necessary tools to analyze the QNM of black holes that reduce to this specific differential equation. The potential (2.5) possesses two irregular singular points at  $z = 0$  and  $z = \infty$ , mirroring the singularity structure of the extremal RN radial equation which we will discuss in the next section.

### 3 Scalar Perturbations of Extremal RN Black Holes

In this section, we explicitly construct the dictionary relating the scalar perturbation of an extremal RN black hole to the quantum SW curve of the SU(2) gauge theory with  $N_f = 2$  fundamental hypermultiplets. We first reduce the radial wave equation to the standard DCHE and subsequently match the physical parameters to the gauge theory parameters.

#### 3.1 Scalar Perturbations in the Extremal Background

The background metric of an extremal RN black hole, where the mass  $M$  equals the electric charge  $Q$ , in standard spherical coordinates is given by

$$ds^2 = -f(r)dt^2 + \frac{dr^2}{f(r)} + r^2(d\theta^2 + \sin^2 \theta d\phi^2), \quad (3.1)$$

where the metric function possesses a double root at the degenerate horizon  $r = Q$ ,

$$f(r) = \left(1 - \frac{Q}{r}\right)^2 = \frac{(r - Q)^2}{r^2}. \quad (3.2)$$

The background electromagnetic gauge potential  $A_\mu$  satisfies  $A_\mu dx^\mu = -\frac{Q}{r} dt$ . We consider a massive charged scalar field  $\Phi$  with mass  $m_p$  and charge  $q$ , governed by the covariant Klein-Gordon equation

$$(\nabla_\mu - iqA_\mu)(\nabla^\mu - iqA^\mu)\Phi - m_p^2\Phi = 0. \quad (3.3)$$

Adopting the standard separation of variables  $\Phi = e^{-i\omega t}R(r)Y_{lm}(\theta, \phi)$ , the radial wave equation becomes

$$\frac{d}{dr} \left[ (r - Q)^2 \frac{d}{dr} \right] R + \left[ \frac{r^2(\omega r - qQ)^2}{(r - Q)^2} - l(l + 1) - m_p^2 r^2 \right] R = 0. \quad (3.4)$$

### 3.2 Reduction to the Double Confluent Heun Equation

To map this radial equation to the normal form of the HE, we first shift the radial coordinate to the horizon by defining  $x = r - Q$ . Subsequently, we redefine the radial function to eliminate the first derivative term by setting  $R(x) = \frac{1}{x}Y(x)$ . This yields a Schrödinger-like equation:

$$\frac{d^2Y}{dx^2} + Q(x)Y = 0, \quad (3.5)$$

where the effective potential  $Q(x)$  is given by

$$Q(x) = \frac{(x + Q)^2[\omega(x + Q) - qQ]^2}{x^4} - \frac{m_p^2(x + Q)^2}{x^2} - \frac{l(l + 1)}{x^2}. \quad (3.6)$$

Expanding  $Q(x)$  in inverse powers of  $x$ , we introduce a dimensionless coordinate  $z = kx$  through the scaling factor

$$k = \frac{1}{Q} \left( \frac{\omega^2 - m_p^2}{(\omega - q)^2} \right)^{\frac{1}{4}}. \quad (3.7)$$

Assuming the physically relevant regime where the frequencies are non-trivial, this scaling remains well-defined. The radial equation then assumes the standard form of the DCHE:

$$\frac{d^2Y}{dz^2} + \left( A_0 + \frac{A_1}{z} + \frac{A_2}{z^2} + \frac{A_3}{z^3} + \frac{A_4}{z^4} \right) Y(z) = 0, \quad (3.8)$$

where the coefficients  $A_i$  are exact algebraic functions of the physical black hole parameters:

$$\begin{aligned}
A_0 &= Q^2(\omega - q)(\omega^2 - m_p^2)^{\frac{1}{2}}, \\
A_1 &= 2Q^2(2\omega^2 - \omega q - m_p^2) \left( \frac{(\omega - q)^2}{\omega^2 - m_p^2} \right)^{\frac{1}{4}}, \\
A_2 &= Q^2(6\omega^2 - 6\omega q + q^2 - m_p^2) - l(l + 1), \\
A_3 &= 2Q^2(2\omega - q)(\omega - q)^{\frac{1}{2}} (\omega^2 - m_p^2)^{\frac{1}{4}}, \\
A_4 &= Q^2(\omega - q)(\omega^2 - m_p^2)^{\frac{1}{2}}.
\end{aligned} \tag{3.9}$$

### 3.3 Branch Selection and the Parameter Dictionary

By matching the algebraic coefficients  $A_i$  of the radial equation with the potential  $\widehat{Q}_2(z)$  of the quantum SW curve, we obtain a system of equations for the gauge theory parameters. Matching the constant term,  $A_0 = -\Lambda_2^2/16$ , yields a quadratic equation for  $\Lambda_2$ , which naturally leads to two distinct mathematical branches.

These two branches differ by a sign flip of the dynamical scale and the mass parameters, while leaving the Coulomb branch parameter  $E$  invariant. To unambiguously identify the correct dictionary for calculating QNM, we must examine the asymptotic behavior of the wave equation.

In black hole perturbation theory, QNM are defined as dissipative resonances. Assuming a time dependence of  $e^{-i\omega t}$ , the physical boundary condition at spatial infinity ( $z \rightarrow \infty$ ) strictly requires a purely outgoing wave. Consequently, the phase must propagate outward, dictating an asymptotic spatial behavior of  $Y \sim e^{+i\kappa z}$ , such that the full wavepacket  $\Phi \sim e^{i(\kappa z - \omega t)}$  travels toward spatial infinity.

Mathematically, as  $z \rightarrow \infty$ , the DCHE reduces to:

$$\frac{d^2 Y}{dz^2} + A_0 Y \sim 0. \tag{3.10}$$

Substituting  $A_0 = -\Lambda_2^2/16$ , the two linearly independent asymptotic solutions are:

$$Y(z) \sim \exp\left(\pm \frac{\Lambda_2}{4} z\right). \tag{3.11}$$

The apparent ambiguity is resolved by considering the standard conventions of mathematical algorithms for Heun functions (e.g., Leaver's continued fraction method or standard numerical packages). To ensure the convergence of the series solutions (e.g., Jaffé expansions) around the irregular singularity, these formalisms typically define the canonical irregular solution by factoring out the decaying exponential:

$$Y_{\text{canonical}}(z) \sim \exp\left(-\frac{\Lambda_2}{4} z\right). \tag{3.12}$$

Notice the explicit negative sign in this mathematical ansatz. If we were to naively adopt the positive branch ( $\Lambda_2 \propto +i\kappa$ ), this canonical solution would correspond to  $e^{-i\kappa z}$ , representing a physically invalid incoming wave.

From a more profound analytic perspective, QNM are not bound states but resonances, corresponding to poles located on the unphysical sheet of the complex energy plane. The parameter  $\Lambda_2$  acts as an effective momentum; flipping its sign precisely maps the solution from the physical sheet (bound states/decaying modes) to the unphysical sheet, correctly capturing the dissipative nature of the black hole radiation. Therefore, the negative branch (3.13) constitutes the exact and physical dictionary for the extremal RN black hole.

After selecting the correct branch, the dictionary is given by:

$$\begin{aligned}
\Lambda_2 &= -4iQ\sqrt{\omega - q}(\omega^2 - m_p^2)^{\frac{1}{4}}, \\
m_1 &= -\frac{iQ(2\omega^2 - \omega q - m_p^2)}{\sqrt{\omega^2 - m_p^2}}, \\
m_2 &= -iQ(2\omega - q), \\
E &= Q^2(6\omega^2 - 6\omega q + q^2 - m_p^2) - l(l + 1) - \frac{1}{4}.
\end{aligned}
\tag{3.13}$$

## 4 Evaluation and Discussion

Having established the exact quantization condition via the SW geometry, we now proceed to calculate the QNM frequencies for the extremal RN black hole. To do so, we substitute the dictionary (3.13) into the quantization condition and solve the resulting non-linear algebraic equation for the complex frequency  $\omega$ . This procedure intrinsically relies on the quantum Matone relation to express the accessory parameter  $E$  as a function of the Coulomb branch parameter  $a$ , the exact expressions for which are detailed in Appendix A.

Since the NS free energy  $\mathcal{F}_{\text{inst}}^{(2)}$  is represented as an infinite series expansion in terms of the dimensionless instanton counting parameter  $(\Lambda_2/a)^2$ , we must truncate the series at a specific instanton order, denoted by  $N_b$ . Furthermore, to analytically continue the series beyond its finite radius of convergence and significantly accelerate the numerical evaluation, we apply Padé approximants to the truncated instanton series.

### 4.1 Neutral Massless Scalar Perturbations

We first focus on neutral massless scalar perturbations ( $q = 0, m_p = 0$ ). The numerical solutions for the least-damped QNM (comprising the fundamental mode  $n = 0$  and the first few overtones  $n = 1, 2$ ) across different angular momentum numbers  $l$  are presented in tables 1–3.

As shown in tables 1–3, our quantization condition yields results that are in agreement with existing numerical results (denoted as “Num”). These benchmark values were obtained by Onozawa et al. [41] utilizing a modified continued fraction method specifically adapted to handle the irregular singularity at the extremal horizon. Following the comparative methodology established in the literature [28], we highlight the matching significant digits between our analytical calculations and the “Num” benchmarks in boldface.

While the continued fraction method is a powerful numerical tool, our geometric approach offers distinct theoretical and analytical advantages. Traditional continued fraction techniques rely on series expansions that naturally fail at the irregular singular point characteristic of the strict extremal limit, necessitating ad-hoc expansions around ordinary points to avoid divergence [41]. In contrast, the SW/QNM correspondence provides an exact, analytically closed quantization condition derived from the non-perturbative NS free energy. Our framework absorbs the singular limits of the spacetime geometry into the well-defined decoupling limit of the gauge theory ( $N_f = 3 \rightarrow N_f = 2$ ). Consequently, rather than serving merely as a numerical root-finding algorithm, our approach elucidates the underlying quantum geometric structure of the QNM spectrum.

For comparison, we also include the third-order WKB results from the same reference [41]. A feature of our gauge-theoretic approach is its systematic improvability. As is visually evident in the tables, the accuracy of the QNM frequencies intrinsically depends on the instanton truncation order  $N_b$ . By increasing the truncation order from  $N_b = 2$  to  $N_b = 12$ , the number of matching bold digits systematically increases, demonstrating a rapid convergence of our numerical roots towards the values. This clearly outperforms the WKB approximation, which inherently stagnates at a fixed approximation error (especially for higher overtones  $n \geq 1$ ). It is important to emphasize that for higher-order instanton corrections, the application of the Padé approximant is essential; without it, the finite radius of convergence of the instanton series would eventually cause the root-finding routine to diverge.

## 4.2 Neutral Massive Scalar Perturbations

The introduction of a non-zero scalar mass  $m_p$  profoundly alters the effective potential at spatial infinity, lifting it from zero to  $m_p^2$ . This asymptotic mass barrier essentially traps low-frequency modes, leading to a phenomenon known as quasi-resonance, where the decay rate of the mode strictly vanishes ( $\text{Im}(\omega) \rightarrow 0$ ). Traditional numerical methods face limitations here: the high-order WKB approximation becomes inaccurate for the fundamental mode ( $l = 0$ ) due to the flattening of the potential barrier, while the continued fraction method struggles at the strictly extremal limit ( $Q = M$ ), because the coalescence of horizons merges the regular singularities into an irregular one, rendering standard recurrence relations divergent.

| $N_b$ | $\omega_0 (n = 0)$                   | $\omega_1 (n = 1)$                   | $\omega_2 (n = 2)$                   |
|-------|--------------------------------------|--------------------------------------|--------------------------------------|
| 2     | <b>0.135942</b> – <b>0.09531379i</b> | 0.104219 – <b>0.3263263i</b>         | <b>0.0905577</b> – <b>0.5722678i</b> |
| 6     | <b>0.133571</b> – <b>0.09579728i</b> | <b>0.0930262</b> – <b>0.3304667i</b> | <b>0.0582712</b> – <b>0.5822183i</b> |
| 10    | <b>0.133460</b> – <b>0.09584264i</b> | <b>0.0929726</b> – <b>0.3306388i</b> | <b>0.0766498</b> – <b>0.5889973i</b> |
| 12    | <b>0.133459</b> – <b>0.09584382i</b> | <b>0.0929558</b> – <b>0.3306619i</b> | <b>0.0754519</b> – <b>0.5885324i</b> |
| WKB   | 0.121090 – 0.103710i                 | 0.091570 – 0.337420i                 | 0.050560 – 0.571640i                 |
| Num   | <b>0.13346</b> – <b>0.095844i</b>    | <b>0.092965</b> – <b>0.33065i</b>    | <b>0.075081</b> – <b>0.58833i</b>    |

**Table 1.** Solutions  $\omega_n$  to the quantization condition for neutral massless scalar perturbations ( $q = 0, m_p = 0$ ) of the extremal RN black hole with angular momentum  $l = 0$ . The matching digits are highlighted in boldface. The integer  $N_b$  denotes the truncation order of the instanton counting series. The WKB and numerical (“Num”) values are taken from Ref. [41] for comparison.

| $N_b$ | $\omega_0 (n = 0)$                   | $\omega_1 (n = 1)$                  | $\omega_2 (n = 2)$                  |
|-------|--------------------------------------|-------------------------------------|-------------------------------------|
| 2     | <b>0.377546</b> – <b>0.09326217i</b> | <b>0.347954</b> – <b>0.2757739i</b> | <b>0.297818</b> – <b>0.4855431i</b> |
| 6     | <b>0.377529</b> – <b>0.08381240i</b> | <b>0.347937</b> – <b>0.2762973i</b> | <b>0.298583</b> – <b>0.4860861i</b> |
| 10    | <b>0.377610</b> – <b>0.08937425i</b> | <b>0.348184</b> – <b>0.2761371i</b> | <b>0.298431</b> – <b>0.4864539i</b> |
| 12    | <b>0.377633</b> – <b>0.08935923i</b> | <b>0.348181</b> – <b>0.2761396i</b> | <b>0.298461</b> – <b>0.4864347i</b> |
| WKB   | 0.375700 – 0.089360i                 | 0.343920 – 0.278280i                | 0.296610 – 0.481450i                |
| Num   | <b>0.37764</b> – <b>0.0893834i</b>   | <b>0.34818</b> – <b>0.27614i</b>    | <b>0.29846</b> – <b>0.48643i</b>    |

**Table 2.** Same as Table 1, but for angular momentum  $l = 1$ .

| $N_b$ | $\omega_0 (n = 0)$                   | $\omega_1 (n = 1)$                  | $\omega_2 (n = 2)$                  |
|-------|--------------------------------------|-------------------------------------|-------------------------------------|
| 2     | <b>0.625186</b> – <b>0.09108756i</b> | <b>0.606390</b> – <b>0.2680631i</b> | <b>0.573375</b> – <b>0.4577315i</b> |
| 6     | <b>0.625179</b> – <b>0.08547868i</b> | <b>0.608213</b> – <b>0.2692497i</b> | <b>0.572839</b> – <b>0.4582304i</b> |
| 10    | <b>0.626367</b> – <b>0.09069463i</b> | <b>0.608265</b> – <b>0.2690701i</b> | <b>0.572847</b> – <b>0.4582082i</b> |
| 12    | <b>0.626027</b> – <b>0.08880593i</b> | <b>0.608207</b> – <b>0.2691114i</b> | <b>0.572863</b> – <b>0.4581931i</b> |
| WKB   | 0.626090 – 0.088730i                 | 0.606770 – 0.269440i                | 0.572540 – 0.457500i                |
| Num   | <b>0.62657</b> – <b>0.088748i</b>    | <b>0.60817</b> – <b>0.26909i</b>    | <b>0.57287</b> – <b>0.45820i</b>    |

**Table 3.** Same as Table 1, but for angular momentum  $l = 2$ .

Our non-perturbative quantization condition successfully resolves these mathematical difficulties, providing an analytic handle on the strictly extremal geometry. To demonstrate its robustness, we first anchor our results at higher multipoles where the WKB approximation is relatively reliable. Considering a massive scalar field with  $m_p = 0.1$  and  $l = 3$  in the strict extremal limit ( $Q = M$ ), we present the convergence behavior of our quantization condition across different instanton truncation orders ( $N_b$ ) in Table 4.

| $N_b$ ( $Q = M$ )         | $\text{Re}(\omega)$ | $-\text{Im}(\omega)$ |
|---------------------------|---------------------|----------------------|
| 2-instanton               | 0.881943            | 0.095893             |
| 6-instanton               | 0.875956            | 0.088647             |
| 10-instanton              | 0.876697            | 0.089865             |
| 12-instanton              | 0.878275            | 0.092589             |
| WKB ( $Q = 0.999M$ ) [46] | $\sim 0.87$ (est.)  | 0.088517             |

**Table 4.** Calculated QNM frequencies for a massive neutral scalar field ( $m_p = 0.1, l = 3, n = 0$ ) in the strict extremal RN limit ( $Q = M$ ) at different instanton truncation orders  $N_b$ . The results are compared with the 3rd-order WKB benchmark at the near-extremal limit ( $Q = 0.999M$ ) from Ref. [46].

As shown in Table 4, our evaluation for the strictly extremal background ( $Q = M$ ) yields results that are consistent with the established WKB estimations. Specifically, our calculated decay rate aligns closely with the third-order WKB benchmark  $\text{Im}(\omega) = 0.088517$  reported by Konoplya [46] for the near-extremal case ( $Q = 0.999M$ ). To the best of our knowledge, this specific data point constitutes the only explicitly reported numerical data available in the literature for a neutral massive scalar field in this particular regime; consequently, our comparative analysis is necessarily restricted to this single value, while keeping in mind that the accuracy of WKB method is limited. Nevertheless, the minor relative difference between the two methods demonstrates a fundamental consistency. This alignment indicates that our exact geometric approach is practically reliable, and our calculated frequencies—which also furnish the real part ( $\text{Re}(\omega) \approx 0.876$ ) typically absent in standard WKB data—can serve as a useful reference for the QNM spectrum in the strict extremal limit.

Besides, our analytic framework allows us to smoothly track the evolution of the fundamental mode ( $l = 0$ ) across a wide range of scalar masses. As illustrated in Figure 1, we present the continuous trajectory of both the imaginary and real parts of the  $l = 0$  mode as  $m_p$  increases. A notable physical feature is observed in Figure 1a: as the dimensionless mass parameter  $m_p$  increases, the decay rate  $-\text{Im}(\omega)$  is non-linearly suppressed and monotonically approaches zero. This continuous trajec-

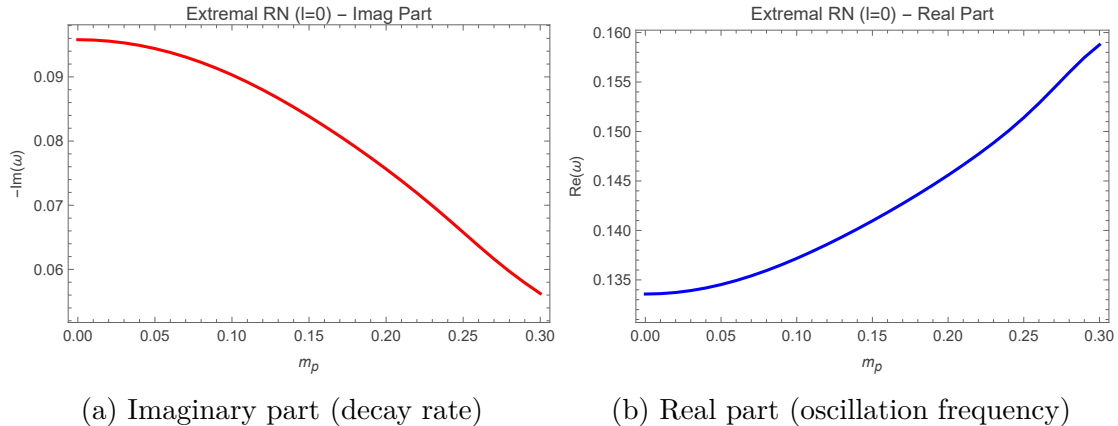


**Figure 1.** The evolution of the fundamental QNM ( $n = 0, l = 0$ ) for a neutral scalar field as a function of the dimensionless mass  $m_p$  in the strict extremal RN limit ( $Q = M$ ). The decay rate strictly approaches zero, explicitly illustrating the transition into the quasi-resonance regime.

tory of the decay rate precisely replicates the physical trend observed by Ohashi and Sakagami [47] for near-extremal black holes ( $Q = 0.99M$ ) using generalized continued fractions. However, our result is obtained analytically at the exact  $Q = M$  limit. Furthermore, our explicit visualization of the real part evolution (Figure 1b) directly complements the parametric complex-plane trajectories presented in earlier numerical literature. Physically, this confirms that for sufficiently large  $m_p$ , the scalar wave is completely confined between the infinite  $AdS_2$  throat near the degenerate horizon and the  $m_p^2$  barrier at spatial infinity. The SW geometry thus captures the cutoff of black hole dissipation, providing an description of quasi-resonances without suffering from the singularity degeneracies that plague standard numerical schemes.

## 5 Conclusion and Outlook

In this paper, we have extended the SW/QNM correspondence to the extremal RN black hole in asymptotically flat spacetime. Due to the coalescence of the inner and outer horizons, the radial perturbation equation naturally maps to the DCHE. Our main analytical result is the exact construction of the dictionary between the scalar perturbations of the extremal RN black hole and the parameters of the quantum  $N_f = 2$  SW curve.

Numerically, we verified the robustness of our quantization condition. For neutral scalar perturbations ( $q = 0$ ), the evaluation of the NS free energy up to the 12-instanton order yielded resonant frequencies consistent with known numerical results. More significantly, for neutral massive scalars ( $m_p \neq 0$ ), our analytic framework successfully tracked the fundamental mode ( $l = 0$ ) into the quasi-resonance regime, explicitly illustrating the cutoff of dissipation ( $\text{Im}(\omega) \rightarrow 0$ ) due to the asymptotic

mass barrier. This demonstrates the method’s capability to resolve the singularity coalescence of the DCHE arising at the strict extremal limit, where standard numerical techniques may face limitations.

Looking ahead, the geometric framework established here paves the way for two possible directions. The first is the calculation of QNM for charged scalar fields, and the second is mathematically accommodating the distinct asymptotic behavior of quasi-bound states. We plan to systematically explore these physically rich spectra in future investigations.

## Acknowledgments

The authors thank Prof. Xian-Hui Ge, Rui-Dong Zhu, Hong-Fei Shu, Yang Lei and Masataka Matsumoto for helpful discussions. K.Z. (Hong Zhang) thanks Prof. Hong Lü for drawing attention to this interesting subject. This work is supported by a classified fund from Shanghai city.

## A Nekrasov-Shatashvili Free Energy for $N_f = 2$

For self-containment, this appendix briefly reviews the exact definitions and the instanton expansion of the NS free energy for the four-dimensional  $\mathcal{N} = 2$  SU(2) gauge theory coupled to  $N_f = 2$  fundamental hypermultiplets. The combinatorial formulations and notation adopted here follow the standard literature, particularly relying on the conventions established in [28].

### A.1 Combinatorial Formulation

The NS limit of the free energy is extracted from the full instanton partition function  $\mathcal{Z}$  by taking the specific  $\Omega$ -background limit  $\epsilon_2 \rightarrow 0$  while keeping  $\epsilon_1 \equiv \hbar$  finite:

$$F_{\text{inst}}^{(N_f)}(a; \mathbf{m}; \Lambda_{N_f}, \hbar) = \lim_{\epsilon_2 \rightarrow 0} \epsilon_2 \log \mathcal{Z}^{(N_f)}(ia, \mathbf{m}, \hbar, \epsilon_2). \quad (\text{A.1})$$

Here, the parameters  $a$ ,  $\mathbf{m} = \{m_1, m_2\}$ , and  $\Lambda_2$  denote the Coulomb branch vacuum expectation value (acting as the corresponding Kähler modulus), the hypermultiplet masses, and the dynamical scale of the theory, respectively.

Based on the standard localization techniques, the general  $\Omega$ -deformed U(2) Nekrasov partition function for  $N_f = 2$  is evaluated as a sum over pairs of Young partitions  $\mathbf{Y} = (Y_1, Y_2)$ :

$$\mathcal{Z}^{(2)}(a; \mathbf{m}; \Lambda_2, \epsilon_1, \epsilon_2) = \sum_{\mathbf{Y}} \left( \frac{\Lambda_2^2}{4} \right)^{\ell(\mathbf{Y})} \mathcal{Z}_{\mathbf{Y}}^{\text{gauge}} \mathcal{Z}_{\mathbf{Y}}^{\text{matter}}, \quad (\text{A.2})$$

where  $\ell(\mathbf{Y}) = |Y_1| + |Y_2|$  counts the total number of boxes in the partition pair. Setting the Coulomb branch parameters to  $\alpha_2 = -\alpha_1 = a$ , the vector multiplet

(gauge) contribution reads:

$$\begin{aligned} \mathcal{Z}_{\mathbf{Y}}^{\text{gauge}} &= \prod_{I,J=1}^2 \prod_{s \in Y_I} \frac{1}{\alpha_I - \alpha_J - \epsilon_1 v_{Y_J}(s) + \epsilon_2 (h_{Y_I}(s) + 1)} \\ &\times \prod_{s \in Y_J} \frac{1}{\alpha_I - \alpha_J + \epsilon_1 (v_{Y_I}(s) + 1) - \epsilon_2 h_{Y_J}(s)}, \end{aligned} \quad (\text{A.3})$$

while the contribution originating from the  $N_f = 2$  fundamental matter multiplets is:

$$\mathcal{Z}_{\mathbf{Y}}^{\text{matter}} = \prod_{k=1}^2 \prod_{I=1}^2 \prod_{(i,j) \in Y_I} \left( \alpha_I + m_k + \left(i - \frac{1}{2}\right) \epsilon_1 + \left(j - \frac{1}{2}\right) \epsilon_2 \right). \quad (\text{A.4})$$

For any specific box  $s = (i, j)$  located within a Young diagram  $Y$ , its arm length  $h_Y(s)$  and leg length  $v_Y(s)$  are given by  $h_Y(s) = y_i - j$  and  $v_Y(s) = y_j^t - i$ , where  $y_i$  and  $y_j^t$  specify the lengths of the  $i$ -th row and the  $j$ -th column, respectively.

## A.2 Full Free Energy and Instanton Expansion

The quantization condition fundamentally relies on the derivative of the complete NS free energy with respect to  $a$ . This full expression systematically incorporates the classical, one-loop, and non-perturbative instanton terms:

$$\begin{aligned} \partial_a \mathcal{F}^{(2)}(a; \mathbf{m}; \Lambda_2, \hbar) &= -4a \log \left( \frac{\Lambda_2}{2\hbar} \right) - \pi \hbar - 2i\hbar \log \left[ \frac{\Gamma \left( 1 + \frac{2ia}{\hbar} \right)}{\Gamma \left( 1 - \frac{2ia}{\hbar} \right)} \right] \\ &- i\hbar \sum_{j=1}^2 \log \left[ \frac{\Gamma \left( \frac{1}{2} + \frac{m_j - ia}{\hbar} \right)}{\Gamma \left( \frac{1}{2} + \frac{m_j + ia}{\hbar} \right)} \right] + \frac{\partial \mathcal{F}_{\text{inst}}^{(2)}(a; \mathbf{m}; \Lambda_2, \hbar)}{\partial a}. \end{aligned} \quad (\text{A.5})$$

To correctly describe the SU(2) gauge theory, the spurious U(1) factor must be decoupled from the U(2) partition function [28]. This decoupling modifies the first instanton correction, yielding the true SU(2) instanton free energy:

$$\mathcal{F}_{\text{inst}}^{(2)}(a; \mathbf{m}; \Lambda_2, \hbar) = F_{\text{inst}}^{(2)}(a; \mathbf{m}; \Lambda_2, \hbar) - \frac{\Lambda_2^2}{8}. \quad (\text{A.6})$$

Evaluating the combinatorial sums, the power series expansion of  $F_{\text{inst}}^{(2)}$  in the dynamical scale  $\Lambda_2$ , evaluated up to  $\mathcal{O}(\Lambda_2^6)$ , explicitly reads:

$$\begin{aligned} F_{\text{inst}}^{(2)}(a; \mathbf{m}; \Lambda_2, \hbar) &= \left( \frac{1}{2} - \frac{(4m_1 m_2)}{2(4a^2 + \hbar^2)} \right) \frac{\Lambda_2^2}{4} \\ &- \frac{\Lambda_2^4}{1024(a^2 + \hbar^2)(4a^2 + \hbar^2)^3} \left( 64a^2(a^4 + 3a^2(m_1^2 + m_2^2) + 5m_1^2 m_2^2) \right. \\ &+ \hbar^6 + 12\hbar^4(a^2 + m_1^2 + m_2^2) + 16\hbar^2(3a^4 + 6a^2(m_1^2 + m_2^2) \\ &\left. - 7m_1^2 m_2^2) \right) + \mathcal{O}(\Lambda_2^6). \end{aligned} \quad (\text{A.7})$$

### A.3 Quantum Mirror Map via Matone Relation

The gauge theoretic parameter  $a$  is implicitly related to the energy eigenvalue  $E$  through the exact quantum mirror map. For  $SU(2)$  theories, this is efficiently encoded by the generalized Matone relation [48]. Specializing to the  $N_f = 2$  case, the exact relation states:

$$E = a^2 - \frac{1}{2}\Lambda_2\partial_{\Lambda_2}\mathcal{F}_{\text{inst}}^{(2)}. \quad (\text{A.8})$$

During the numerical procedure, we invert this relation perturbatively using the explicit expansion (A.7). This provides the necessary analytic continuation to express  $a$  strictly as a function of the physical spectral variables  $(E, m_1, m_2, \Lambda_2)$ , which is subsequently implemented into the Bohr-Sommerfeld quantization condition.

## References

- [1] N. Seiberg and E. Witten, *Electric - magnetic duality, monopole condensation, and confinement in  $\mathcal{N} = 2$  supersymmetric Yang-Mills theory*, *Nucl. Phys. B* **426** (1994) 19–52, [[hep-th/9407087](#)].
- [2] N. Seiberg and E. Witten, *Monopoles, Duality and Chiral Symmetry Breaking in  $\mathcal{N} = 2$  Supersymmetric QCD*, *Nucl. Phys. B* **431** (1994) 484–550, [[hep-th/9408099](#)].
- [3] P. C. Argyres and M. R. Douglas, *New phenomena in  $SU(3)$  supersymmetric gauge theory*, *Nucl. Phys. B* **448** (1995) 93–126, [[hep-th/9505062](#)].
- [4] J. A. Minahan and D. Nemeschansky, *An  $N=2$  superconformal fixed point with  $E_6$  global symmetry*, *Nucl. Phys. B* **482** (1996) 142–152, [[hep-th/9608047](#)].
- [5] A. Klemm, W. Lerche, S. Theisen and S. Yankielowicz, *Simple singularities and  $N=2$  supersymmetric Yang-Mills theory*, *Phys. Lett. B* **344** (1995) 169–175, [[hep-th/9411048](#)].
- [6] R. Donagi and E. Witten, *Supersymmetric Yang-Mills theory and integrable systems*, *Nucl. Phys. B* **460** (1996) 299–334, [[hep-th/9510101](#)].
- [7] N. A. Nekrasov, *Seiberg-Witten prepotential from instanton counting*, *Adv. Theor. Math. Phys.* **7** (2003) 831–864, [[hep-th/0206161](#)].
- [8] A. Gorsky, I. Krichever, A. Marshakov, A. Mironov and A. Morozov, *Integrability and Seiberg-Witten exact solution*, *Phys. Lett. B* **355** (1995) 466–474, [[hep-th/9505035](#)].
- [9] A. Mironov and A. Morozov, *Nekrasov Functions and Exact Bohr-Sommerfeld Integrals*, *JHEP* **04** (2010) 040, [[0910.5670](#)].
- [10] L. F. Alday, D. Gaiotto and Y. Tachikawa, *Liouville Correlation Functions from Four-dimensional Gauge Theories*, *Lett. Math. Phys.* **91** (2010) 167–197, [[0906.3219](#)].
- [11] N. Wyllard,  *$A(N-1)$  conformal Toda field theory correlation functions from conformal  $N=2$   $SU(N)$  quiver gauge theories*, *JHEP* **11** (2009) 002, [[0907.2189](#)].

- [12] T. Regge and J. A. Wheeler, *Stability of a Schwarzschild singularity*, *Phys. Rev.* **108** (1957) 1063–1069.
- [13] F. J. Zerilli, *Effective potential for even parity Regge-Wheeler gravitational perturbation equations*, *Phys. Rev. Lett.* **24** (1970) 737–738.
- [14] E. Berti, V. Cardoso and A. O. Starinets, *Quasinormal modes of black holes and black branes*, *Class. Quant. Grav.* **26** (2009) 163001, [[0905.2975](#)].
- [15] R. A. Konoplya and A. Zhidenko, *Quasinormal modes of black holes: From astrophysics to string theory*, *Rev. Mod. Phys.* **83** (2011) 793–836, [[1102.4014](#)].
- [16] K. D. Kokkotas and B. G. Schmidt, *Quasinormal modes of stars and black holes*, *Living Rev. Rel.* **2** (1999) 2, [[gr-qc/9909058](#)].
- [17] LIGO SCIENTIFIC, VIRGO collaboration, B. P. Abbott et al., *Observation of Gravitational Waves from a Binary Black Hole Merger*, *Phys. Rev. Lett.* **116** (2016) 061102, [[1602.03837](#)].
- [18] LIGO SCIENTIFIC, VIRGO collaboration, B. P. Abbott et al., *Tests of General Relativity with GW150914*, *Phys. Rev. Lett.* **116** (2016) 221101, [[1602.03841](#)].
- [19] O. Dreyer, B. Kelly, B. Krishnan, L. S. Finn, D. Garrison and R. Lopez-Aleman, *Black hole spectroscopy: Testing general relativity through gravitational wave observations*, *Class. Quant. Grav.* **21** (2004) 787–804, [[gr-qc/0309007](#)].
- [20] E. Berti, A. Sesana, E. Barausse, V. Cardoso and K. Belczynski, *Spectroscopy of Kerr black holes with Earth- and space-based interferometers*, *Phys. Rev. Lett.* **117** (2016) 101102, [[1605.09286](#)].
- [21] M. Isi, M. Giesler, W. M. Farr, M. A. Scheel and S. A. Teukolsky, *Testing the no-hair theorem with GW150914*, *Phys. Rev. Lett.* **123** (2019) 111102, [[1905.00869](#)].
- [22] N. Yunes and X. Siemens, *Gravitational-Wave Tests of General Relativity with Ground-Based Detectors and Pulsar Timing Arrays*, *Living Rev. Rel.* **16** (2013) 9, [[1304.3473](#)].
- [23] E. Berti, K. Yagi and N. Yunes, *Extreme Gravity Tests with Gravitational Waves from Compact Binary Coalescences: (I) Inspiral-Merger*, *Gen. Rel. Grav.* **50** (2018) 46, [[1801.03208](#)].
- [24] H.-P. Nollert, *Quasinormal modes: the characteristic 'sound' of black holes and neutron stars*, *Class. Quant. Grav.* **16** (1999) R159–R216.
- [25] E. W. Leaver, *An Analytic representation for the quasi-normal modes of Kerr black holes*, *Proc. Roy. Soc. Lond. A* **402** (1985) 285–298.
- [26] S. Iyer and C. M. Will, *Black Hole Normal Modes: A WKB Approach. 1. Foundations and Application of a Higher Order WKB Analysis of Potential Barrier Scattering*, *Phys. Rev. D* **35** (1987) 3621.
- [27] R. A. Konoplya, *Quasinormal behavior of the d-dimensional Schwarzschild black hole and higher order WKB approach*, *Phys. Rev. D* **68** (2003) 024018, [[gr-qc/0303052](#)].

- [28] G. Aminov, A. Grassi and Y. Hatsuda, *Black Hole Quasinormal Modes and Seiberg-Witten Theory*, *Annales Henri Poincaré* **23** (2022) 1951–1977, [[2006.06111](#)].
- [29] M. Bianchi, D. Consoli, A. Grillo and J. F. Morales, *QNMs of branes, BHs and fuzzballs from quantum SW geometries*, *Phys. Lett. B* **824** (2022) 136837, [[2105.04245](#)].
- [30] M. Bianchi, D. Consoli, A. Grillo and J. F. Morales, *More on the SW-QNM correspondence*, *JHEP* **01** (2022) 024, [[2109.09804](#)].
- [31] Y. Hatsuda, *Quasinormal modes of black holes and Borel summation*, *Phys. Rev. D* **101** (2020) 024008, [[1906.07232](#)].
- [32] S. A. Teukolsky, *Perturbations of a rotating black hole. I. Fundamental equations for gravitational, electromagnetic, and neutrino-field perturbations*, *Astrophys. J.* **185** (1973) 635–647.
- [33] A. Litvinov, S. Lukyanov, N. Nekrasov and A. Zamolodchikov, *Classical Conformal Blocks and Painlevé VI*, *JHEP* **07** (2014) 144, [[1309.4700](#)].
- [34] P. P. Fiziev, *Exact Solutions of Regge-Wheeler Equation and Quasi-Normal Modes of Compact Objects*, *Class. Quant. Grav.* **23** (2006) 2447–2468, [[gr-qc/0509039](#)].
- [35] X.-H. Ge, M. Matsumoto and K. Zhang, *Massive vector field perturbations in the Schwarzschild spacetime from supersymmetric gauge theory*, *Phys. Rev. D* **112** (2025) 046024, [[2502.15627](#)].
- [36] P. Yang, Y.-R. Wang and K. Zhang, *Extended Heun Hierarchy in Quantum Seiberg-Witten Geometry*, [2601.05204](#).
- [37] D. Senjaya and S. Ponglertsakul, *The extreme Reissner-Nordström Black Hole: New exact solutions to the Klein-Gordon equation with minimal coupling*, *Annals of Physics* **473** (2025) 169898, [[2405.07579](#)].
- [38] O. Gamayun, N. Iorgov and O. Lisovyy, *How instanton combinatorics solves Painlevé VI, V and III's*, *J. Phys. A* **46** (2013) 335203, [[1302.1832](#)].
- [39] Y. Hatsuda, *Quasinormal modes of Kerr-de Sitter black holes via the Heun function*, *Class. Quant. Grav.* **38** (2021) 025015, [[2006.08957](#)].
- [40] N. A. Nekrasov and S. L. Shatashvili, *Quantization of Integrable Systems and Four Dimensional Gauge Theories*, in *XVIIth International Congress on Mathematical Physics*, pp. 265–289, 2010. [0908.4052](#). DOI.
- [41] H. Onozawa, T. Mishima, T. Okamura and H. Ishihara, *Quasinormal modes of maximally charged black holes*, *Phys. Rev. D* **53** (1996) 7033–7040, [[gr-qc/9603021](#)].
- [42] A. Mironov and A. Morozov, *Nekrasov Functions and Exact Bohr-Sommerfeld Integrals*, *JHEP* **04** (2010) 040, [[0910.5670](#)].
- [43] G. Bonelli, C. Iossa, D. P. Lichtig and A. Tanzini, *Exact solution of Kerr black hole perturbations via  $CFT_2$  and instanton counting: Greybody factor, quasinormal modes, and Love numbers*, *Phys. Rev. D* **105** (2022) 044047, [[2105.04483](#)].

- [44] X.-H. Ge, M. Matsumoto and K. Zhang, *Duality between Seiberg-Witten Theory and Black Hole Superradiance*, *JHEP* **05** (2024) 336, [[2402.17441](#)].
- [45] Y. Lei, H. Shu, K. Zhang and R.-D. Zhu, *Quasinormal modes of C-metric from SCFTs*, *JHEP* **02** (2024) 140, [[2308.16677](#)].
- [46] R. A. Konoplya, *Massive charged scalar field in a Reissner-Nordstrom black hole background: Quasinormal ringing*, *Phys. Lett. B* **550** (2002) 117–120, [[gr-qc/0210105](#)].
- [47] A. Ohashi and M.-a. Sakagami, *Massive quasi-normal mode*, *Class. Quant. Grav.* **21** (2004) 3973–3984, [[gr-qc/0407009](#)].
- [48] M. Matone, *Instantons and recursion relations in  $\mathcal{N} = 2$  SUSY gauge theory*, *Phys. Lett. B* **357** (1995) 342–348, [[hep-th/9506102](#)].